



Doping of Monolayer Transition-Metal Dichalcogenides via Physisorption of Aromatic Solvent Molecules

Ye Wang, Amine Slassi, Marc-Antoine Stoeckel, Simone Bertolazzi, Jérôme Cornil, David Beljonne, Paolo Samorì

► To cite this version:

Ye Wang, Amine Slassi, Marc-Antoine Stoeckel, Simone Bertolazzi, Jérôme Cornil, et al.. Doping of Monolayer Transition-Metal Dichalcogenides via Physisorption of Aromatic Solvent Molecules. *Journal of Physical Chemistry Letters*, 2019, 10 (3), pp.540-547. <10.1021/acs.jpclett.8b03697>. <hal-02056928>

HAL Id: hal-02056928

<https://hal.science/hal-02056928v1>

Submitted on 4 Mar 2019

HAL is a multi-disciplinary open access archive for the deposit and dissemination of scientific research documents, whether they are published or not. The documents may come from teaching and research institutions in France or abroad, or from public or private research centers.

L'archive ouverte pluridisciplinaire **HAL**, est destinée au dépôt et à la diffusion de documents scientifiques de niveau recherche, publiés ou non, émanant des établissements d'enseignement et de recherche français ou étrangers, des laboratoires publics ou privés.



HAL Authorization

Doping of Monolayer Transition Metal Dichalcogenides via Physisorption of Aromatic Solvent Molecules

*Ye Wang,¹ Amine Slassi,² Marc-Antoine Stoeckel,¹ Simone Bertolazzi,¹ Jérôme Cornil,²
David Beljonne,^{2*} Paolo Samorì^{1*}*

¹University of Strasbourg, CNRS, ISIS UMR 7006, 8 allée Gaspard Monge, F-67000, Strasbourg, France.

²Laboratory for Chemistry of Novel Materials, Université de Mons, Place du Parc 20, 7000 Mons, Belgium

Corresponding Author

* Paolo Samorì samori@unistra.fr ; David Beljonne david.beljonne@umons.ac.be

ABSTRACT Two-dimensional (2D) transition metal dichalcogenides (TMDs) recently emerged as novel materials displaying a wide variety of physico-chemical properties that render them unique scaffolds for high-performance (opto)electronics. The controlled physisorption of molecules on the TMD surface is a viable approach to tune their optical and electronic properties. Solvents, made of small aromatic molecules, are frequently employed for the cleaning of the 2D materials or as “dispersant” for their chemical functionalization with larger (macro)molecules, without considering their potential key effect in locally modifying the characteristics of 2D materials. In this work, we demonstrate how the electronic and optical properties of mechanically exfoliated monolayer of MoS₂ and WSe₂ are modified when physically interacting with small aromatic molecules of common solvents. Low-

temperature photoluminescence (PL) spectra recorded at 78 K revealed that physisorbed benzene derivatives could modulate the charge carrier density in monolayer TMDs, hence affecting the switching between neutral exciton and trion (charged exciton). By combining experimental evidences with DFT calculations, we confirm that charge transfer doping on TMDs depends not only on difference in chemical potential between molecules and 2D materials, but also on the thermodynamic stability of physisorption. Our results provide unambiguous evidence of the great potential of optical and electrical tuning of monolayer MoS₂ and WSe₂ by physisorption of small aromatic solvent molecules, which is highly relevant both for fundamental studies and more device applied purposes.

Keywords: transition metal dichalcogenides, aromatic molecules, doping, photoluminescence, Density Functional Theory.

TOC GRAPHICS

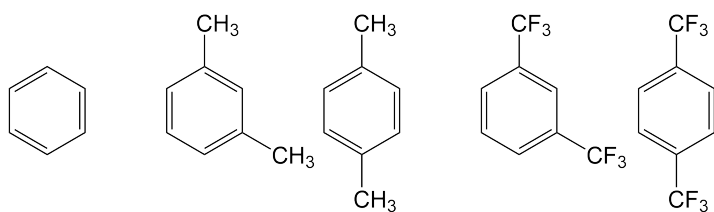
KEYWORDS transition metal dichalcogenides, aromatic molecules, doping, photoluminescence, Density Functional Theory.

TEXT

During the last decade, two-dimensional (2D) materials have attracted remarkable attention owing to their unique physical and chemical properties. Among them, transition metal dichalcogenides (TMDs) are semiconducting systems that exhibit an indirect-to-direct bandgap transition from bulk to monolayer, large exciton binding energies, and inversion symmetry breaking, which are attractive for a large range of applications from (opto)electronics to valleytronics¹⁻⁶. The largest surface-to-volume

ratio in the crystal structure of monolayer TMDs makes them extremely sensitive to changes in the environment.⁷ In this regard, the simple physisorption of atoms and molecules represents a powerful method to modulate their optical and electrical properties.⁷⁻⁸

Highly polar physisorbed molecules including TCNQ and NADH,⁹ hydrazine,¹⁰ benzene viologen,¹¹ have been utilized for the chemical doping of monolayer TMDs. Interactions between these molecules and TMDs induce charge transfer, thus modifying the Fermi level and tuning the electronic and optical properties of the material. In monolayer TMDs, strong electron-hole Coulomb interactions enable the formation of stable optically generated excitons at room temperature;¹²⁻¹³ these excitons are building blocks for the generation of many-body bound states such as electron-bound exciton (negative trion) or hole-bound exciton (positive trion)¹⁴⁻¹⁵. Accordingly, electron/hole concentrations modified by physisorbed molecules effectively influence the formation of excitons and trions in TMDs.



Scheme 1. Chemical formula of benzene, m-xylene, p-xylene, 1,3-bis(trifluoro)methylbenzene (1,3-TFMB), and 1,4-bis(trifluoromethyl)benzene (1,4-TFMB).

Although a great effort has been devoted to the non-covalent functionalization of monolayer TMDs via molecular physisorption to improve fundamental properties¹⁶ such as photoluminescence tuning,^{9-10, 17-18} electron/hole doping^{19,20} and device contact improvement,²¹ the simple interaction of a functionalized benzene ring (being

frequently a fragment of solvent molecules) and monolayer TMDs has not yet been fully unraveled.²² Despite the fact that typical solvent molecules are seemingly considered as inert media, aromatic molecules have been proved to cause n- or p-doping with distinct functional groups through π - π interactions with graphene.²³ Unfortunately, similar studies on TMDs have not yet been reported. To gain a comprehensive understanding over the effect of physisorbed molecules on monolayer TMDs, we focused here our attention to the benzene and its derivatives depicted in **Scheme 1**, i.e. benzene, m-xylene, p-xylene, 1,3-bis(trifluoro)methylbenzene (1,3-TFMB) and 1,4-bis(trifluoromethyl)benzene (1,4-TFMB)) as aromatic molecules, and MoS₂ and WSe₂ as representative TMD monolayers acting as platforms for physisorption. The functionality of aromatic molecules is therefore modified through simple substitution in the *meta* and *para* position with either more apolar methyl (-CH₃) or more polar trifluoromethyl (-CF₃) groups. The melting point, boiling point and total dipole moment of each molecule are listed in **Table S1**. Importantly, benzene, m-xylene and p-xylene are commonly used as solvents to dissolve complex organic molecules for functionalization of 2D materials and for device fabrication. These aromatic solvents could be unintentionally physisorbed on 2D materials resulting in changes in physical and chemical properties. Thus, understanding the effect of these molecules on monolayer TMDs is a crucial issue to be addressed not only for unveiling molecule-TMD interactions but also for device optimization. We reveal here on the occurrence of charge transfer between physisorbed molecules and monolayer TMDs, leads to change in electron/hole density and trion/exciton intensity ratio. Through low-temperature photoluminescence (PL) measurements performed at 78 K corroborated with Density Functional Theory calculations, we quantify n or p nature of doping for each molecule deposited on monolayer TMDs. Our results

provide a text-book proof-of-concept on the use of physisorbed aromatic molecules on single-layer TMDs to dope the 2D material in a controlled fashion.

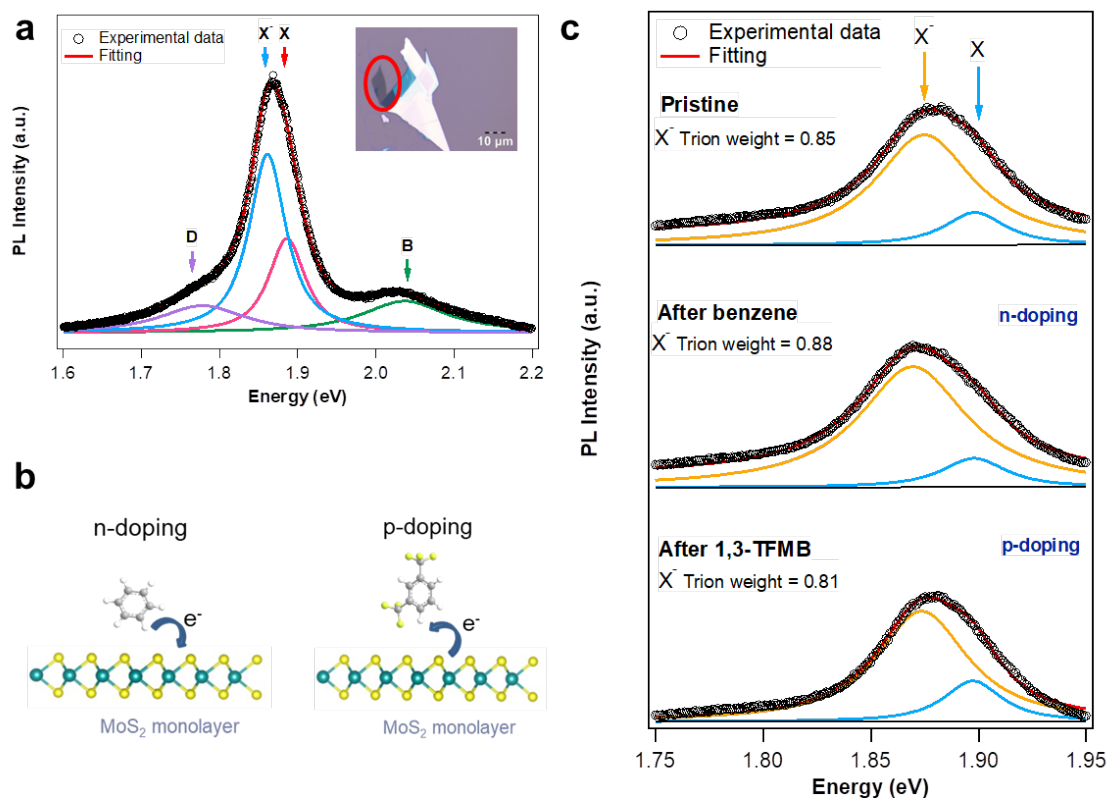


Figure 1. **a)** Photoluminescence spectra of monolayer MoS₂ at 78 K (inset: optical image of as exfoliated monolayer MoS₂ highlighted with a red circle). **b)** Molecular representation of charge transfer between physisorbed aromatic molecules and monolayer MoS₂. **c)** Photoluminescence spectra of monolayer MoS₂ before and after physisorption of benzene and 1,3-TFMB with calculated X⁻ trion weight.

The photoluminescence behavior of monolayer MoS₂ is known to be strongly temperature dependent.²⁴⁻²⁶ Typical PL spectrum of monolayer MoS₂ at 78 K recorded in N₂ atmosphere is shown in **Figure 1 (a)**. It exhibits four components in the range of 1.6 to 2.2 eV: a neutral A exciton (X) at ~1.88 eV and a negatively charged A trion (X⁻) at ~1.90 eV, a B exciton (B) at ~2.05 eV and a defect-induced emission (D) at ~1.75 eV. The A excitons (X and X⁻) are blue-shifted of 23 meV compared to room temperature due to the bandgap enlargement upon decreasing the temperature.²⁴ Temperature dependent studies on the photoluminescence of monolayer MoS₂ (**Figure S1** in the

Supporting information) reveals that localized emission caused by excitons bounded with defects (D) appears below 100 K. It is fair to indicate that such D peak is not observed in every flakes of our experiment likely because of the difference in defect density generated by mechanical exfoliation.

The physisorption of benzene and its derivatives (i.e. benzene, m-xylene, p-xylene, 1,3-bis(trifluoro)methylbenzene (1,3-TFMB) and 1,4-bis(trifluoromethyl)benzene (1,4-TFMB)) as aromatic molecules onto monolayer MoS₂ (**Figure 1 (b)**) is explored by monitoring the photoluminescence spectra. Such study provides evidence for the occurrence of chemical doping as revealed by major changes in PL emission intensity and shape.⁹ Representative PL spectra of monolayer MoS₂ tuned by aromatic molecules at 78 K are portrayed in **Figure 1. a)** Photoluminescence spectra of monolayer MoS₂ at 78 K (inset: optical image of as exfoliated monolayer MoS₂ highlighted with a red circle. **b)** Molecular representation of charge transfer between physisorbed aromatic molecules and monolayer MoS₂. **c)** Photoluminescence spectra of monolayer MoS₂ before and after physisorption of benzene and 1,3-TFMB with calculated X- trion weight. (c) whereas the spectra, and related fitting, for MoS₂ with all kinds of physisorbed molecules is displayed in **Figure S3** in the Supporting Information. We focus our attention on the A peak that tracks the population of trion (X) and neutral exciton (X). Given that at 78 K all aromatic molecules investigated are in their solid phase, the chemical doping process might differ from those reported in previous studies carried out at room temperature.^{9-10, 17-18} Our data reveal that upon treatment with benzene, the spectral weight of trion increases whereas the use of 1,3-TFMB induces a decrease in the trion weight. Such effects are caused by changes in charge carrier density in monolayer MoS₂ induced by molecular doping. When monolayer MoS₂ is n-doped, the increase in electron density promotes the formation of negatively charged trion.

Conversely, p-doping enables the recombination of neutral excitons into positively charged trion. The trion weight can be quantified as:

$$\gamma^- = \frac{I_{X^-}}{I_{total}} = \frac{I_{X^-}}{I_{X^-} + I_X} \quad (1)$$

where γ^- is the negative trion weight of monolayer MoS₂, I_{X^-} is the area of negative trion peak, I_X is the area of neutral exciton peak and I_{total} is the area of total photoluminescence intensity. Therefore, we calculate the trion weight change ($\Delta\gamma^-$). $\Delta\gamma^- > 0$, indicates an increase in electron density upon molecular physisorption, implying a n-doping effect. Conversely $\Delta\gamma^- < 0$, denotes a decrease in electron density upon molecular physisorption, corresponding to p-doping.

To explore the origin of the trion weight change ($\Delta\gamma^-$), we have discussed different mechanisms which led to the exclusion of dipolar effects and the activation of defect-induced photoluminescence, as shown in Supporting notes in Supporting Information. This discussion made it possible to demonstrate that the observed induced doping in the TMDs is due to charge transfer between molecules and 2D materials. The trion weight change ($\Delta\gamma^-$) quantifies the ability of doping, in this specific case of MoS₂ as a result of the physisorption of the molecular monolayer, as determined by PL measurements. In the simplest approximation, when two species *A* and *B* (here the solvent molecules and the MoS₂ solid) with chemical potentials $\mu_A \neq \mu_B$ are brought into close contact, electron density *N* flows from the high-potential to the low-potential system until equilibration is reached: ²⁷

$$\Delta N = \frac{\mu_A - \mu_B}{\eta_A + \eta_B} \quad (2)$$

where η_A and η_B are the chemical hardness of *A* and *B*, respectively. To understand the difference in values of $\Delta\gamma^-$ resulting from the physisorption of different

molecules, we have calculated the chemical potential and hardness values of monolayer MoS₂ and the investigated aromatic molecules.²⁸ In the frontier molecular orbital framework and using a finite difference approximation, these write:

$$\mu = \frac{1}{2}(\varepsilon_{hole} + \varepsilon_{electron}); \eta = \frac{1}{2}(\varepsilon_{electron} - \varepsilon_{hole}) \quad (3)$$

Where ε_{hole} ($\varepsilon_{electron}$) denotes the energy of the molecular HOMO (LUMO) level for the solvent and the energy of the top of the valence (conduction) band for the 2D solid.

As shown in **Figure 2**, fluorinated molecules have a smaller chemical potential due to the electron-withdrawing character of -CF₃ groups. The chemical potential of monolayer MoS₂ is calculated to be -5.1 eV, which is closely above that of -5.15 and -5.19 eV for 1,3-TFMB and 1,4-TFMB, respectively. Therefore, electrons tend to transfer from MoS₂ to 1,3-TFMB and 1,4-TFMB, so that electron density is decreased in monolayer MoS₂, resulting in p-doping effect. In contrast, benzene (-3.84 eV), m-xylene (-3.50 eV) and p-xylene (-3.47 eV) have higher chemical potentials than monolayer MoS₂, hence it is easier to transfer electron from the former to the latter, leading to n-doping of the 2D layer. While the chemical hardness weighted difference in chemical potential between aromatic molecules explains the type of doping of MoS₂, the quantitative agreement is limited. In other words, the sign of the calculated ΔN in Eq. (2) is consistent with the measured $\Delta \gamma^-$, but the trend with the nature of the solvent is only qualitative (see **Table S2** in Supporting Information). For example, benzene has smaller chemical potential than xylenes but it gives larger trion weight change; 1,3-TFMB and 1,4-TFMB have much smaller chemical potential difference than other molecules but $\Delta \gamma^-$ are comparable to benzene and xylenes. This is likely because of the thermodynamic stability drive to certain configurations of the self-

assembled molecules on the surface of MoS₂, possibly sourcing a surface electrostatic potential, together with other effects not included in the simple model (hybridization with and electronic polarization in the solid). To better appraise these effects, we have assessed the charge transfer taking place from the solvents to the MoS₂ (WSe₂) sheet upon adsorption by applying the Bader charge analysis to the equilibrated interfaces ²⁹. The calculated charge transfer matches the trend of $\Delta\gamma^-$ much better than the chemical potential based model (**Figure 2**).

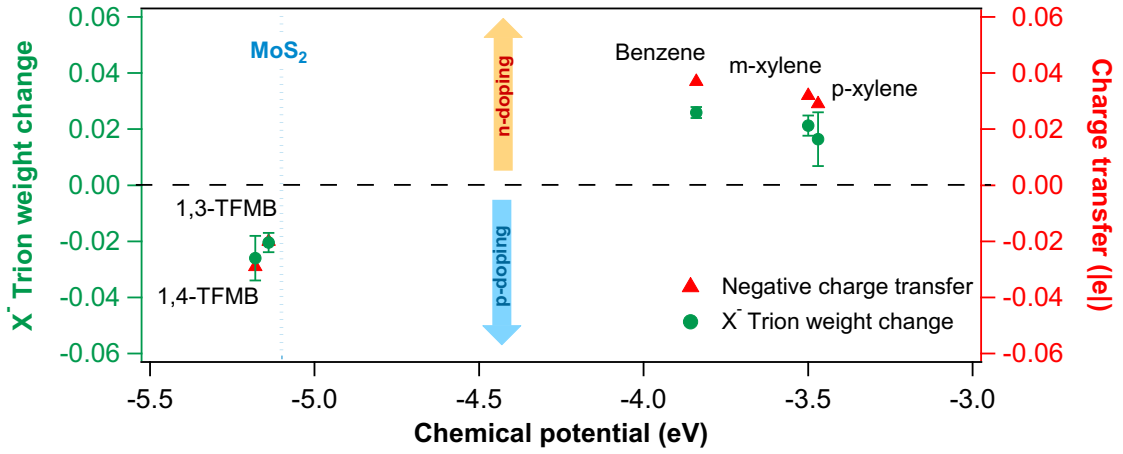


Figure 2. X⁻ trion weight change and calculated Bader charge transfer (red) by physisorption of aromatic molecules from low-temperature PL measurement of MoS₂ (green) as a function of chemical potential. Fluorinated molecules (1,3-TFMB and 1,4-TFMB) possessing lower chemical potential are easier to accept electrons from monolayer MoS₂; in contrast, non-fluorinated molecules (benzene, p-xylene and m-xylene) with higher chemical potential donate electrons to monolayer MoS₂.

The correlation of $\Delta\gamma^-$ and charge transfer value can be estimated by mass action model ³⁰:

$$\frac{N_X n_{el}}{N_{X^-}} = \left(\frac{4m_X m_e}{\pi \hbar^2 m_{X^-}} \right) k_B T \exp\left(-\frac{E_b}{k_B T}\right) \quad (4)$$

where N_X and N_{X^-} are the population of excitons (X) and trions (X⁻). n_{el} is the electron density and E_b is the binding energy of trion (~20 meV). T is the temperature

(78 K). m_X , m_{X^-} and m_e are effective masses of exciton, trion and electron respectively. Considering $m_e \approx 0.35m_0$ and $m_h \approx 0.45m_0$, m_X and m_{X^-} can be calculated as $m_X = m_e + m_h = 0.8m_0$, and $m_{X^-} = 2m_e + m_h = 1.15m_0$. Hence, the trion weight can be expressed as

$$\frac{I_{X^-}}{I_{total}} = \frac{\frac{\gamma_{tr} N_{X^-}}{\gamma_{ex} N_X}}{1 + \frac{\gamma_{tr} N_{X^-}}{\gamma_{ex} N_X}} \approx \frac{1.5 \cdot 10^{-15} n_{el}}{1 + 1.5 \cdot 10^{-15} n_{el}} \quad (5)$$

where γ_{tr} and γ_{ex} are radiative decay rates of trion and exciton, respectively. **Figure 3** demonstrates a good correspondence between the electron density change obtained from experimental data and the charge transfer predicted by DFT calculations, as the electron density change of monolayer MoS₂ after the physisorption of aromatic molecules is linearly proportional to charge transfer value per molecule. By carefully excluding the doping effect from air atmosphere, our measurements shows that the modulation of charge density by solvent trace in monolayer MoS₂ is largely decreased to 10¹¹/cm² compared to previous studies that attain 10¹³/cm².³⁰ Therefore, it is possible to estimate the number of physisorbed molecules on the surface of monolayer MoS₂ by considering

$$\Delta n_{el} \cdot |e| = n_{mol} \cdot \Delta \sigma^- \quad (6)$$

where Δn_{el} is the change in electron density, $|e|$ is the absolute value of elementary charge, n_{mol} is the number of molecules adsorbed per unit area (cm²) and $\Delta \sigma^-$ is the negative charge transfer value. The estimated number of adsorbed molecules for each chemical is listed in

Table 1. It is clear that xylenes have the smaller number of adsorbed molecules, whereas fluorinated molecules tend to self-assemble more densely on the surface of the MoS₂. This might be attributed to the preference of Coulomb interaction between electron-withdrawing -CF₃ group and the intrinsically n-doped monolayer MoS₂. We

have also studied at a theoretical level how charge transfer from the physisorbed molecules to the TMD monolayer is influenced by varying the density of molecules, inter-layer distance and inclination angle between molecules and monolayer MoS_2 , as discussed in the Supporting notes in the Supporting information.

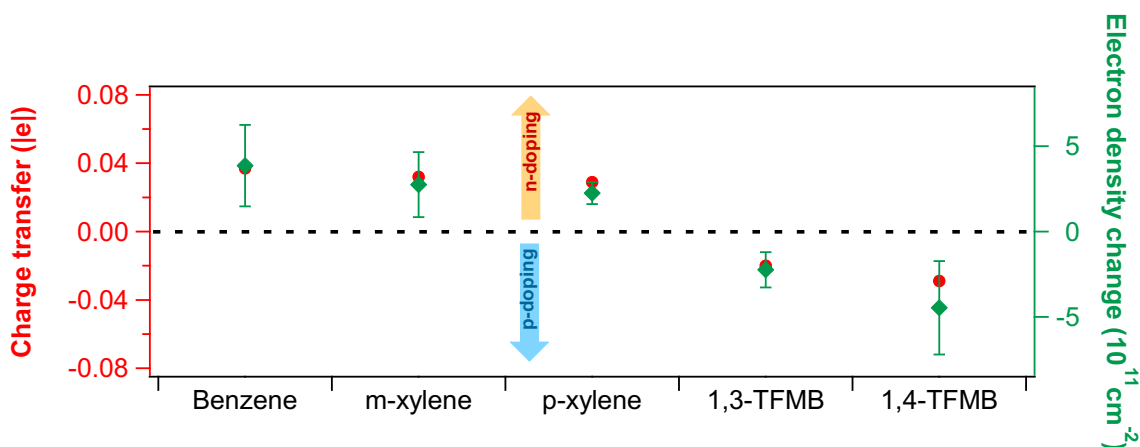


Figure 3. Electron density change (green) after physisorption on MoS_2 of each aromatic molecule, as calculated by mass action model and provided by a DFT/Bader charge analysis (red).

	Benzene	m-Xylene	p-Xylene	1,3-TFMB	1,4-TFMB
Number of physisorbed molecules ($10^{13}/\text{cm}^2$)	1.04	0.86	0.77	1.12	1.54

Table 1 Estimated number of physisorbed aromatic molecules on monolayer MoS_2 calculated from electron density change and transferred charge.

In contrast to monolayer MoS_2 , the photoluminescence behavior of monolayer WSe_2 exhibits multiple possibilities for trion recombination. At low temperature, the coexistence of neutral excitons and positively charged excitons or negatively charged excitons and biexcitons is observed by changing temperature (4 K, 10 K, 30 K, 60 K) and device structure.³¹⁻³³ To investigate the influence of aromatic molecules deposited on monolayer WSe_2 , we first study here its excitonic characteristics at 78 K on SiO_2 substrate. The temperature dependence of monolayer WSe_2 is similar to MoS_2 whereby,

upon decreasing the temperature, the exciton peak is blue-shifted. Defect-induced emissions appear below 200 K as multiple peaks in the range of 1.60 eV to 1.65 eV in which the intensity is dependent on the quality of the flakes. Moreover, at room temperature, a single excitonic peak at 1.66 eV is observed. Below 100 K, this peak is split into two independent components at ~ 1.72 eV and ~ 1.70 eV (**Figure S2** in the Supporting Information).

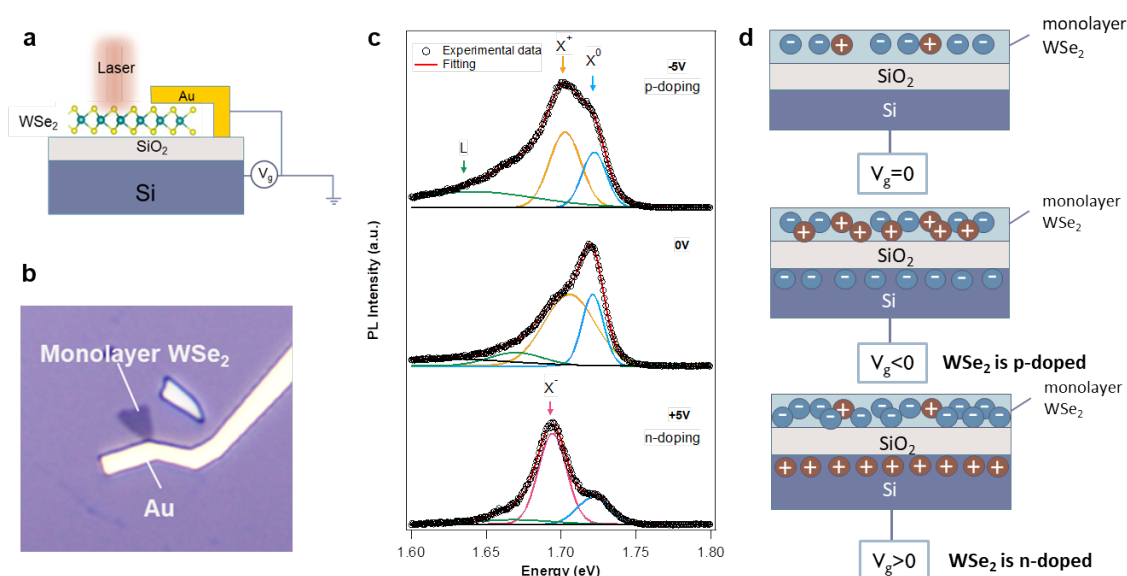


Figure 4. Gate-induced photoluminescence of monolayer WSe₂. **a)** Schematic representation of the device for gate-induced photoluminescence in monolayer WSe₂, and **b)** its corresponding optical image. **c)** PL spectra of monolayer WSe₂ at 78 K under -5, 0, +5V, demonstrating the recombination of neutral exciton (X⁰) and positive trion (X⁺) at 0V and -5V, and the existence of neutral exciton (X⁰) and negative trion (X⁻) at +5V. **d)** Modulation of charge carrier by gating. The change in carrier density results in electrostatic doping on monolayer WSe₂ and affects the recombination of positive or negative trions.

To assign the origin of these two excitonic components, field-effect devices were fabricated by E-beam lithography to induce electrical tunable doping. **Figure 4(a)** and **(b)** portray the schematic and optical image of the device, respectively. As displayed in the scheme in **Figure 4(d)**, by adding a gate voltage on FET device, it is possible to modulate charge carrier density in WSe₂ monolayers, and therefore to tune the

proportion of excitons and trions. Upon applying negative gate voltage, electrons in monolayer WSe₂ are attracted to the ground via the gold electrode, the electron density in the material is therefore largely decreased and neutral excitons tend to capture excess holes to form positive trion. On the contrary, when applying a positive gate voltage, more electrons are attracted to the channel, therefore negative trion recombination is facilitated. **Figure 4(c)** shows the PL spectra of monolayer WSe₂ at 78 K under -5 V, 0 V and +5 V gate voltage, respectively. At 0 V, apart from the peak at ~1.65 eV, two other peaks, namely trion at ~1.70 eV and exciton at ~1.72 eV are observed. At -5 V, the intensity of the trion peak increases. Considering the increase in hole density by increasing negative gate voltage, we assign this peak as positive trion (two holes and one electron combined). This also implies that our material is intrinsically p-doped even after annealing, which is inconsistent with former works where either protection layer of h-BN was added or the experiment was performed at lower temperature³². At +5 V, when more electrons are injected into monolayer WSe₂, the negative trion (two electrons and one hole combined) emission at ~1.69 eV dominates. We extract the binding energy of positive trion and negative trion at 78 K to be 17~22 meV and 31~40 meV respectively by calculating the difference of trion emission energy and neutral exciton energy. We have also observed quantum-confined Stark effect by applying higher gate voltage and a substrate-induced hysteresis in PL mapping under small gating steps, yet this is beyond the scope of this work.

After studying the peak position of each type of exciton emission in our experimental conditions, we focus our attention on the effect of chemical doping on monolayer

WSe₂. With no gate voltage applied to the flake, we only discuss the neutral exciton and positive trion. We quantify the positive trion as

$$\gamma^+ = \frac{I_{X^+}}{I_{total}} = \frac{I_{X^+}}{I_X + I_{X^+}} \quad (7)$$

where γ^+ is the positive trion weight of monolayer WSe₂, I_{X^+} is the area of positive trion peak, and I_X is the area of neutral exciton peak and I_{total} is the area of total photoluminescence intensity. Therefore, we calculate the trion weight change ($\Delta\gamma^+$) to evaluate the charge transfer doping of molecules on monolayer WSe₂.

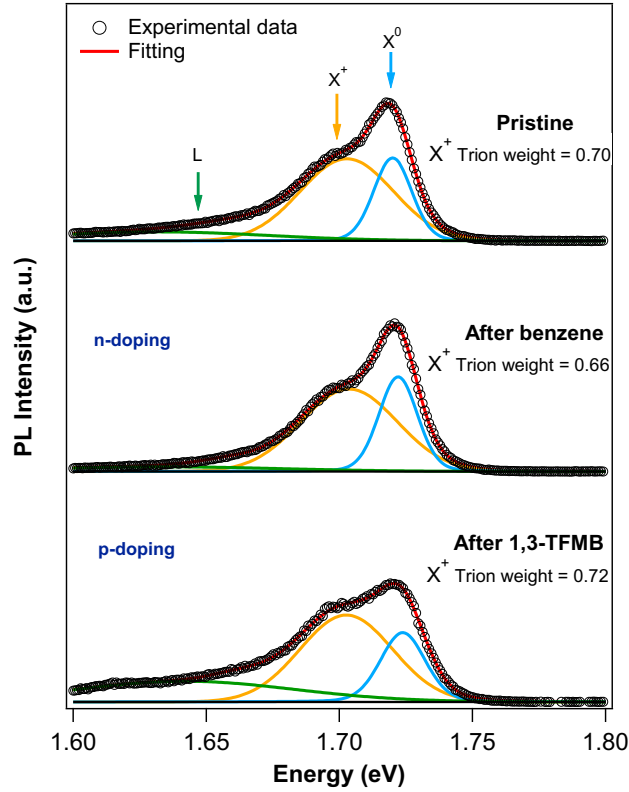


Figure 5. Photoluminescence spectra of monolayer WSe₂ before and after physisorption of benzene, and 1,3-TFMB with calculated X⁺ trion weight.

Figure 5 shows typical fitted PL spectra before and after doping with aromatic molecules at 78 K. The spectral weight change of trion induced by benzene indicates n-doping and that 1,3-TFMB is a p-dopant. For other aromatic molecules, we find

similar type of doping as monolayer MoS₂ (detailed PL spectra in **Figure S4** of Supporting Information). To elucidate the consistency of doping, we have calculated the chemical potential of monolayer WSe₂ to be -4.33 eV, which is nearly 1 eV above the fluorinated molecules but still 1 eV lower than the other molecules, suggesting that the charge transfer direction between the molecules and monolayer WSe₂ should be the same as in MoS₂. Both calculated charge transfers and trion weight changes reveal that benzene has the largest n-doping ability and that 1,4-TFMB p-dopes the monolayer WSe₂ the most. Both xylenes have trivial influence on carrier density change in monolayer WSe₂. (**Figure 6**)

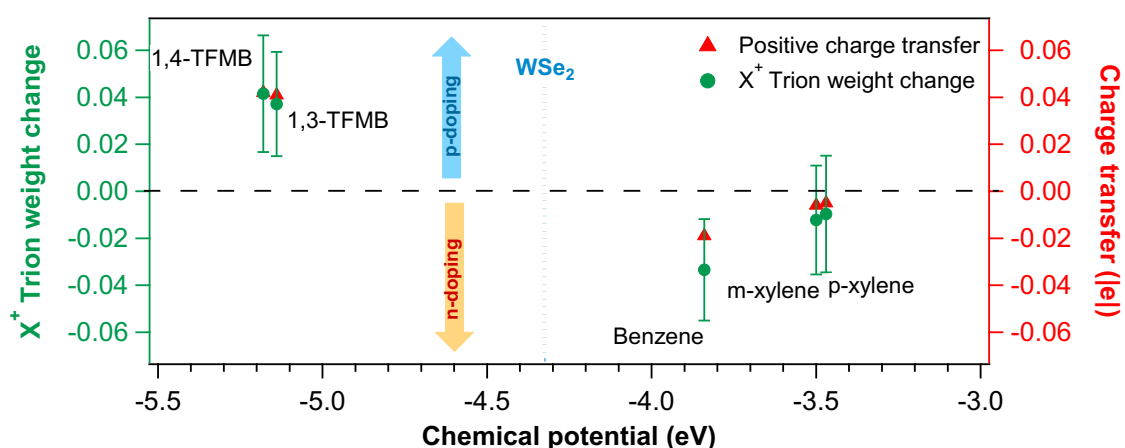


Figure 6. X⁺ trion weight change and calculated DFT/Bader charge transfer (red) by physisorption of aromatic molecules from low-temperature PL measurements of monolayer WSe₂ (green) as a function of chemical potential. Fluorinated molecules (1,3-TFMB and 1,4-TFMB) possessing lower chemical potential are more prone to accept electrons from monolayer MoS₂; in contrast, non-fluorinated molecules (benzene, p-xylene and m-xylene) with higher chemical potential donate electrons to monolayer WSe₂.

In summary, our spectroscopic investigation provides unambiguous evidence of the full potential of the physisorption of small aromatic molecules on MoS₂ and WSe₂ to tune their opto-electronic properties via charge transfer. The PL study performed at 78 K demonstrated for the first time that tunable chemical doping can be achieved on

both 2D materials through a subtle choice of simple aromatic molecules and their dosing on the surface. In particular, while fluorinated aromatics determined a p-doping, an n-doping was observed for the other methyl-substituted molecules. The calculated charge transfer of fluorinated solvent molecules on MoS₂ could be comparable to traditional organic p-dopants tetracyanoquinodimethane (TCNQ) and tetracyanoethylene (TCNE), while typical n-dopants tetrathiafulvalene (TTF) and benzene viologen (BV) could donate electrons beyond the ability of aromatic solvents.¹⁷ Charge carrier modulation by optical response is found to be two orders of magnitude lower in charge carrier density than previous studies at room temperature in air^{9, 30} by freezing the system at low temperature in inert atmosphere. The combined experimental analyses and DFT calculations utilized in this study represents a novel technique for estimating the density of physisorbed molecules in 2D surfaces. Furthermore, we have investigated for the first time the gate-tunable photoluminescence and defined binding energy of both positive and negative trions of monolayer WSe₂ at 78K through field-effect transistor.

Our results clearly indicate that care should be taken when choosing the solvent for the cleaning of the 2D materials or as “dispersant” for their chemical functionalization with larger (macro)molecules, since it can introduce strong electronic effects like doping. On the other hand, solvent molecules are clearly multifunctional systems since they both act as dispersant for the 2D materials and can enable the tuning of their optoelectronic properties.

Overall, our findings are instrumental both for fundamental and more applicative studies as many relevant solvents consist of small aromatic molecules, which therefore cannot be considered as inert media in the processing, but rather as a powerful tool for tuning the TMD properties and device optimization.

EXPERIMENTAL SECTION

Sample preparation. Monolayer MoS₂ and WSe₂ flakes were mechanically exfoliated from commercially available molybdenum disulfide (Furuchi, Japan) and tungsten disulfide (HQ Graphene) crystals using the scotch tape method. The flakes were transferred onto SiO₂ (90 nm) / Si substrate, and their thickness was monitored by optical microscope combined with Raman spectroscopy and Atomic Force Microscopy (AFM). The samples were thermally annealed at 200 °C inside a vacuum chamber to desorb atmospheric adsorbates. Then, they were no longer exposed to air after the annealing and were characterized only under inert atmosphere (N₂-filled glovebox). Anhydrous solvents from Sigma Aldrich were opened in glovebox filled with N₂. To exclude the dielectric screening caused by environmental changes after depositing solvent molecules, we drop-cast each solvent molecule on monolayer TMDs, and spin-dried at 2000 RPM for 60 s to guarantee the presence of limited number molecules physisorbed on the surface of the TMD.

Low-temperature photoluminescence spectroscopy. Photoluminescence spectra were recorded in inert atmosphere (N₂) by using a Renishaw inVia spectrometer equipped with 532 nm laser in aid of Linkam TP95 temperature controller. Samples were mounted in the glovebox and immediately measured after annealing to avoid exposure to air. The spectra were taken at different temperature, spanning from room temperature (298 K) down to 78 K. The excitation power was kept below 1 mW to avoid local heating damage effects. The wavenumber (energy) resolution amounted to ~1 meV.

Device fabrication and electrical characterization. Back-gated FETs were fabricated on thermally oxidized heavily *n*-doped silicon substrates (Fraunhofer Institute IPMS, $\rho_{\text{Si}} \sim 0.001 \text{ } \Omega\cdot\text{cm}$, $t_{\text{ox}} = 90 \text{ nm}$) by means of E-beam lithography with polymethyl methacrylate (PMMA) resists, thermal evaporation of Au (80 nm) and lift-off in acetone. Devices were annealed in high vacuum ($\sim 10^{-7}$ mbar) overnight at 200 °C (Plassys

ME400B). Electrical characterization was carried out at room temperature under N₂ atmosphere (glovebox) with source-measurement units from Keithley (model 2636A).

Computational details. Our theoretical calculations were performed using density functional theory with the projector-augmented wave (PAW) scheme, as implemented in the Vienna Ab-Initio Simulation Package (VASP).³⁴⁻³⁵ The exchange-correlation potentials were treated by Perdew-Burke-Ernzerhof (PBE) ³⁶ parametrization of the generalized gradient approximation (GGA) and the kinetic energy cutoff for basis set was 600 eV. Van der Waals interactions were taken into account using Grimme's semiempirical DFT-D2 corrections.³⁷ To model the physisorption of solvents on MoS₂ (WSe₂) monolayer, a 5×5×1 supercell was constructed and a vacuum of 25 Å thickness was used to avoid any physical interactions in the stacking direction. The first Brillouin zone integration was performed using 2×2×1 and 4×4×1 Monkhorst-Pack k-point mesh ³⁸ for geometry optimizations and electronic structure calculations, respectively. The integral atomic positions were fully relaxed according to the Hellmann–Feynman forces until the residual forces and total energy difference remain below 1 meV/Å and 10⁻⁵ eV, respectively.

ASSOCIATED CONTENT

The Supporting Information is available free of charge on the ACS Publications website at DOI:

AUTHOR INFORMATION

YW, SB and PS conceived the experiment. YW worked on sample preparation, device fabrication, optical and electrical characterization. YW, MAS and SB analyzed the data. AS, JC and DB performed the modeling work. YW and PS co-wrote the paper. All

authors discussed the results and contributed to the interpretation of data as well as to editing the manuscript.

ACKNOWLEDGEMENTS

We thank Y. Zhao (ISIS) for valuable discussions and precious support. Device fabrication was carried out in part at the nanotechnology facility eFab (IPCMS, Strasbourg). The authors are thankful to S. Siegwald for assistance with microfabrication. We acknowledge funding from the M-ERA.NET project MODIGLIANI, the European Commission through the Graphene Flagship (GA-696656) and the Marie-Curie IEF MULTI2DSWITCH (GA-700802), as well as the the Agence Nationale de la Recherche through the Labex projects CSC (ANR- 10-LABX-0026 CSC) and NIE (ANR-11-LABX-0058 NIE) within the Investissement d'Avenir program (ANR-10-120 IDEX-0002-02), and the International Center for Frontier Research in Chemistry (icFRC). The work in Mons is supported by FNRS/F.R.S. JC and DB are FNRS Research Directors.

REFERENCES

- (1) Akinwande, D.; Petrone, N.; Hone, J. Two-dimensional flexible nanoelectronics. *Nat. Commun.* **2014**, *5*, 5678.
- (2) Fiori, G.; Bonaccorso, F.; Iannaccone, G.; Palacios, T.; Neumaier, D.; Seabaugh, A.; Banerjee, S. K.; Colombo, L. Electronics Based on Two-Dimensional Materials. *Nat. Nanotechnol.* **2014**, *9* (10), 768-779.
- (3) Mak, K. F.; Shan, J. Photonics and optoelectronics of 2D semiconductor transition metal dichalcogenides. *Nat. Photonics* **2016**, *10*, 216.
- (4) Hu, Y.; Huang, Y.; Tan, C.; Zhang, X.; Lu, Q.; Sindoro, M.; Huang, X.; Huang, W.; Wang, L.; Zhang, H. Two-dimensional transition metal dichalcogenide nanomaterials for biosensing applications. *Mater. Chem. Frontiers* **2017**, *1* (1), 24-36.
- (5) Li, S.-L.; Tsukagoshi, K.; Orgiu, E.; Samorì, P. Charge transport and mobility engineering in two-dimensional transition metal chalcogenide semiconductors. *Chem. Soc. Rev.* **2016**, *45* (1), 118-151.
- (6) Yan, W.; Txoperena, O.; Llopis, R.; Dery, H.; Hueso, L. E.; Casanova, F. A two-dimensional spin field-effect switch. *Nat. Commun.* **2016**, *7*, 13372.

- (7) Anichini, C.; Czepa, W.; Pakulski, D.; Aliprandi, A.; Ciesielski, A.; Samori, P. Chemical sensing with 2D materials. *Chem. Soc. Rev.* **2018**, *47*, 4860-4908.
- (8) Bertolazzi, S.; Gobbi, M.; Zhao, Y.; Backes, C.; Samori, P. Molecular chemistry approaches for tuning the properties of two-dimensional transition metal dichalcogenides. *Chem. Soc. Rev.*, **2018**, *47*, 6845-6888.
- (9) Mouri, S.; Miyauchi, Y.; Matsuda, K. Tunable photoluminescence of monolayer MoS₂ via chemical doping. *Nano Lett.* **2013**, *13* (12), 5944-5948.
- (10) Lee, I.; Rathi, S.; Li, L.; Lim, D.; Khan, M. A.; Kannan, E. S.; Kim, G.-H. Non-degenerate n-type doping by hydrazine treatment in metal work function engineered WSe₂ field-effect transistor. *Nanotechnology* **2015**, *26* (45), 455203.
- (11) Kiriya, D.; Tosun, M.; Zhao, P.; Kang, J. S.; Javey, A. Air-stable surface charge transfer doping of MoS₂ by benzyl viologen. *J. Am. Chem. Soc.* **2014**, *136* (22), 7853-7856.
- (12) Splendiani, A.; Sun, L.; Zhang, Y. B.; Li, T. S.; Kim, J.; Chim, C. Y.; Galli, G.; Wang, F. Emerging Photoluminescence in Monolayer MoS₂. *Nano Lett.* **2010**, *10* (4), 1271-1275.
- (13) Mak, K. F.; Lee, C.; Hone, J.; Shan, J.; Heinz, T. F. Atomically Thin MoS₂: A New Direct-Gap Semiconductor. *Phys. Rev. Lett.* **2010**, *105* (13).
- (14) Ross, J. S.; Wu, S.; Yu, H.; Ghimire, N. J.; Jones, A. M.; Aivazian, G.; Yan, J.; Mandrus, D. G.; Xiao, D.; Yao, W. Electrical control of neutral and charged excitons in a monolayer semiconductor. *Nat. Commun.* **2013**, *4*, 1474.
- (15) Tongay, S.; Zhou, J.; Ataca, C.; Liu, J.; Kang, J. S.; Matthews, T. S.; You, L.; Li, J.; Grossman, J. C.; Wu, J. Broad-range modulation of light emission in two-dimensional semiconductors by molecular physisorption gating. *Nano Lett.* **2013**, *13* (6), 2831-6.
- (16) Gobbi, M.; Orgiu, E.; Samori, P. "When 2D Materials Meet Molecules: Opportunities and Challenges of Hybrid Organic/Inorganic van der Waals Heterostructures. *Adv. Mater.* **2018**, *30*, 1706103.
- (17) Jing, Y.; Tan, X.; Zhou, Z.; Shen, P. W. Tuning electronic and optical properties of MoS₂ monolayer via molecular charge transfer. *J. Mater. Chem. A* **2014**, *2* (40), 16892-16897.
- (18) Han, H. V.; Lu, A. Y.; Lu, L. S.; Huang, J. K.; Li, H.; Hsu, C. L.; Lin, Y. C.; Chiu, M. H.; Suenaga, K.; Chu, C. W.; Kuo, H. C.; Chang, W. H.; Li, L. J.; Shi, Y. Photoluminescence enhancement and structure repairing of monolayer MoSe₂ by hydrohalic acid treatment. *ACS Nano* **2016**, *10* (1), 1454-1461.
- (19) de la Rosa, C. J. L.; Phillipson, R.; Teyssandier, J.; Adisojoso, J.; Balaji, Y.; Huyghebaert, C.; Radu, I.; Heyns, M.; De Feyter, S.; De Gendt, S. Molecular doping of MoS₂ transistors by self-assembled oleylamine networks. *Appl. Phys. Lett.* **2016**, *109* (25), 253112.
- (20) Kang, D. H.; Dugasani, S. R.; Park, H. Y.; Shim, J.; Gnappareddy, B.; Jeon, J.; Lee, S.; Roh, Y.; Park, S. H.; Park, J. H. Ultra-low Doping on Two-Dimensional Transition Metal Dichalcogenides using DNA Nanostructure Doped by a Combination of Lanthanide and Metal Ions. *Sci. Rep.* **2016**, *6*, 20333.

- (21) Fang, H.; Chuang, S.; Chang, T. C.; Takei, K.; Takahashi, T.; Javey, A. High-performance single layered WSe₂ p-FETs with chemically doped contacts. *Nano Lett.* **2012**, *12* (7), 3788-3792.
- (22) Fisher, A.; Blöchl, P. Adsorption and scanning-tunneling-microscope imaging of benzene on graphite and MoS₂. *Phys. Rev. Lett.* **1993**, *70* (21), 3263.
- (23) Dong, X.; Fu, D.; Fang, W.; Shi, Y.; Chen, P.; Li, L. J. Doping single - layer graphene with aromatic molecules. *Small* **2009**, *5* (12), 1422-1426.
- (24) Korn, T.; Heydrich, S.; Hirmer, M.; Schmutzler, J.; Schüller, C. Low-temperature photocarrier dynamics in monolayer MoS₂. *Appl. Phys. Lett.* **2011**, *99* (10), 102109.
- (25) Lanzillo, N. A.; Birdwell, A. G.; Amani, M.; Crowne, F. J.; Shah, P. B.; Najmaei, S.; Liu, Z.; Ajayan, P. M.; Lou, J.; Dubey, M.; Nayak, S. K.; O'Regan, T. P. Temperature-dependent phonon shifts in monolayer MoS₂. *Appl. Phys. Lett.* **2013**, *103* (9), 093102.
- (26) Mak, K. F.; He, K. L.; Lee, C.; Lee, G. H.; Hone, J.; Heinz, T. F.; Shan, J. Tightly bound trions in monolayer MoS₂. *Nat. Mater.* **2013**, *12* (3), 207-211.
- (27) Crispin, X.; Geskin, V.; Crispin, A.; Cornil, J.; Lazzaroni, R.; Salaneck, W. R.; Bredas, J.-L. Characterization of the interface dipole at organic/metal interfaces. *J. Am. Chem. Soc.* **2002**, *124* (27), 8131-8141.
- (28) Pearson, R. G. The electronic chemical potential and chemical hardness. *J. Mol. Struct.: THEOCHEM* **1992**, *255*, 261-270.
- (29) Tang, W.; Sanville, E.; Henkelman, G. A grid-based Bader analysis algorithm without lattice bias. *J. Phys. Cond. Matter.* **2009**, *21* (8), 084204.
- (30) Choi, J.; Zhang, H.; Du, H.; Choi, J. H. Understanding solvent effects on the properties of two-dimensional transition metal dichalcogenides. *ACS Appl. Mater. Interfaces* **2016**, *8* (14), 8864-8869.
- (31) Ross, J. S.; Klement, P.; Jones, A. M.; Ghimire, N. J.; Yan, J.; Mandrus, D.; Taniguchi, T.; Watanabe, K.; Kitamura, K.; Yao, W. Electrically tunable excitonic light-emitting diodes based on monolayer WSe₂ p-n junctions. *Nat. Nanotechnol.* **2014**, *9* (4), 268.
- (32) Jones, A. M.; Yu, H.; Ghimire, N. J.; Wu, S.; Aivazian, G.; Ross, J. S.; Zhao, B.; Yan, J.; Mandrus, D. G.; Xiao, D. Optical generation of excitonic valley coherence in monolayer WSe₂. *Nat. Nanotechnol.* **2013**, *8* (9), 634.
- (33) You, Y.; Zhang, X.-X.; Berkelbach, T. C.; Hybertsen, M. S.; Reichman, D. R.; Heinz, T. F. Observation of biexcitons in monolayer WSe₂. *Nat. Phys.* **2015**, *11* (6), 477.
- (34) Kresse, G.; Furthmüller, J. Efficient iterative schemes for ab initio total-energy calculations using a plane-wave basis set. *Phys. Rev. B* **1996**, *54* (16), 11169.
- (35) Kresse, G. G. Kresse and D. Joubert, *Phys. Rev. B* **59**, 1758 (1999). *Phys. Rev. B* **1999**, *59*, 1758.
- (36) Perdew, J. P.; Burke, K.; Ernzerhof, M. Generalized gradient approximation made simple. *Phys Rev Lett* **1996**, *77* (18), 3865.

- (37) Grimme, S. Semiempirical GGA - type density functional constructed with a long - range dispersion correction. *J. Comput. Chem.* **2006**, 27 (15), 1787-1799.
- (38) Monkhorst, H. J.; Pack, J. D. Special points for Brillouin-zone integrations. *Phys. Rev. B* **1976**, 13 (12), 5188.